

# Quantitative Analysis of the Effective Functional Structure in Yeast Glycolysis

Jesus M. Cortes<sup>1</sup> and Ildefonso M. De la Fuente<sup>2,3</sup>

**1 DECSAI: Departamento de Ciencias de la Computacion e Inteligencia Artificial.**

**Universidad de Granada, E-18071 Granada. Spain. E-mail: jcortes@decsai.ugr.es**

**2 Instituto de Parasitologia y Biomedicina Lopez-Neyra. CSIC. E-18100 Granada. Spain.**

**E-mail: mtpmadei@ehu.es**

**3 Corresponding author**

## Abstract

Yeast glycolysis is considered the prototype of dissipative biochemical oscillators. In cellular conditions, under sinusoidal source of glucose, the activity of glycolytic enzymes can display either periodic, quasiperiodic or chaotic behavior. In order to quantify the functional connectivity for the glycolytic enzymes in dissipative conditions we have analyzed different catalytic patterns using the non-linear statistical tool of Transfer Entropy. The data were obtained by means of a yeast glycolytic model formed by three delay differential equations where the enzymatic speed functions of the irreversible stages have been explicitly considered. These enzymatic activity functions were previously modeled and tested experimentally by other different groups. In agreement with experimental conditions, the studied time series corresponded to a quasi-periodic route to chaos. The results of the analysis are three-fold: first, in addition to the classical topological structure characterized by the specific location of enzymes, substrates, products and feedback regulatory metabolites, an effective functional structure emerges in the modeled glycolytic system, which is dynamical and characterized by notable variations of the functional interactions. Second, the dynamical structure exhibits a metabolic invariant which constrains the functional attributes of the enzymes. Finally, in accordance with the classical biochemical studies, our numerical analysis reveals in a quantitative manner that the enzyme phosphofructokinase is the key-core of the metabolic system, behaving for all conditions as the main source of the effective causal flows in yeast glycolysis.

## Author Summary

The understanding of the effective functionality that governs the enzymatic self-organized processes in cellular conditions is a crucial topic in the post-genomic era. A number of measures have been proposed for the functionality and correlations between biochemical time series. However, functional correlations do not imply effective connectivity and most synchronization measures do not distinguish between causal and non-causal interactions. In recent studies, Transfer Entropy (TE) has been proposed as a rigorous, robust and self-consistent method for the causal quantification of the functional information flow among nonlinear processes. Here, we have used TE to establish the effective functional connectivity of yeast glycolysis under dissipative conditions. Concretely, we have applied this method for a quantification of how much the temporal evolution of the activity of one enzyme helps to improve the future prediction of another. In the enzymatic activities, the oscillatory patterns of the metabolic products might have causal information which can be appropriately read-out by the TE. We have performed numerical studies of yeast glycolysis under dissipative conditions and found the emergence of a new kind of dynamical functional structure, characterized by changing connectivity flows and a metabolic invariant that constrains the activity of the irreversible enzymes.

## Introduction

Yeast glycolysis is one of the most studied dissipative pathways of the cell; it was the first metabolic system in which spontaneous oscillations were observed [1,2], and the study of these rhythms allowed the construction of the first dynamic model where the kinetics of an enzyme was explicitly considered [3,4]. More concretely, the main instability-generating mechanism in the yeast glycolysis is based on the self-catalytic regulation of the enzyme phosphofructokinase [3,5,6].

Glycolysis is the central pathway of glucose degradation which is implied in relevant metabolic processes, such as the maintenance of cellular redox states, the provision of ATP for membrane pumps and protein phosphorylation, biosynthesis, etc; and its activity is linked to a high variety of important cellular processes, e.g., glycolysis has a long history in cancer cell biology [7] and cell proliferation [8], there is a correlation between brain aerobic glycolysis and Amyloid- $\beta$  plaque deposition which might precede the clinical manifestations of the Alzheimer disease [9], the glycolytic inhibition abrogates epileptogenesis [10], and glycolysis is also related with oxidative stress [11] and apoptosis [12].

Over the last 30 years a large number of different studies focused on different molecular mechanisms allowing for the emergency of self-organized glycolytic patterns [13–18]. Nevertheless, despite the intense advance of the knowledge of these metabolic structure, we still lack a quantitative description in cellular conditions of the effective functional structure and the causal effects among the enzymes.

In this paper, to go a next step further in the understanding of the relationship between the classical topological structure and functionality we have analyzed the effective connectivity of yeast glycolysis, which in inter-enzyme interactions accounts for the influence that the activity of one enzyme has on the future of another [19–23].

For this purpose, we considered a yeast glycolytic model described by a system of three delay-differential equations in which there is an explicit consideration of the speed functions of the three irreversible enzymes hexokinase, phosphofructokinase and pyruvatekinase. These enzymatic activity functions were previously modeled and tested experimentally by other different groups [3,24,25].

We have obtained time series of enzymatic activity under different sources of the glucose input flux. The data corresponded to a typical quasi-periodic route to chaos which is in agreement with experimental conditions [26]. The dynamics of the glycolytic system changes substantially trough this route, which allows for a better comparison of the enzymatic processes in periodic, quasi-periodic and chaotic

conditions.

Using the non-linear analysis techniques such as Transfer Entropy [27] and Mutual Information [28], we have analyzed the glycolytic series and quantified the effective connectivity of the enzymes.

The results show that in the numerical analysis of yeast glycolysis, under dissipative conditions, a effective functional structure emerges which is characterized by changing connectivity flows and a metabolic invariant that constraints the activity of the irreversible enzymes.

## Results

The monitoring of the fluorescence of NADH in glycolyzing baker's yeast under sinusoidal glucose input flux, have shown that quasi-periodic time patterns are common at low amplitudes of the input and for high amplitudes chaotic behaviours emerge [29, 30].

In order to simulate these metabolic processes, the system is considered under periodic input flux with a sinusoidal source of glucose  $S = S_0 + A \sin(\omega t)$ . Assuming the experimental value of  $S_0 = 6\text{mM/h}$  [31], after dividing by  $K_{m2}$  (the Michaelis constant of phosphofructokinase, see for more details Materials and Methods) we have obtained the normalized input flux  $S_0 = 0.033$  Hz.

Under these conditions, a wide range of different types of dynamic patterns can emerge as a function of the control parameter, hereafter the amplitude  $A$  of the sinusoidal glucose input flux [26, 32, 33]. In particular, it is observed a quasi-periodic route to chaos (cf. left panel in Fig. 2); thus for  $A = 0.001$  the biochemical oscillator exhibits a periodic pattern (Figure 2a). An increment of the amplitude to  $A = 0.005$  provokes a Hopf bifurcation generating another fundamental frequency, as a consequence, quasi-periodic behaviors emerge (Figure 2b). Above  $A = 0.021$ , complex quasi-periodic oscillations appear (Figure 2c). After a new Hopf bifurcation the originated dynamical behavior is not particularly stable and small perturbations produce deterministic chaos ( $A = 0.023$ , Figure 2d), as predicted by Ruelle and Takens [34]. This route is in agreement with experimental conditions [26].

To go a next step further in the understanding of the relationship between the classical topological structure and effective functionality we have analyzed by means of non-linear statistical tools the catalytic patterns belonging to this scenario to chaos, and for each transition represented in the Figure 2 we have obtained three time series corresponding to the variables  $\alpha$ ,  $\beta$  and  $\gamma$  (12 in total), which denote respectively the normalized concentrations of glucose-6-phosphate, fructose 1-6-bisphosphate and pyruvate.

## Effective functionality

Transfer Entropy (TE) quantifies the reduction in uncertainty that one variable has on its own future when adding another. This measure allows for a calculation of the functional influence in terms of effective connectivity between two variables [27]. The analysis of the glycolytic data by means of the TE method are shown in Table I. The 4D vectors in square brackets correspond to the results obtained for the 4 different amplitudes of the considered glucose input flux,  $A=[0.001;0.005;0.021;0.023]$ .

The values of functional influence are ranging in  $0.58 \leq TE \leq 1.00$ , with mean= 0.79 and standard deviation=0.12, what indicates in general terms a high effective connectivity in the enzymatic system. The minimum value 0.58 corresponded to the causality flow between  $E_3$  and  $E_2$  when a simple periodic behavior emerges. However, the functional connectivity from  $E_2$  to  $E_3$  shows the maximum value, achieved in all considered conditions of the glucose input flux.

The glycolytic effective connectivity is illustrated in the right panel of Fig. 2. The arrows width is proportional to the TE between pairs of enzymes. The values change trough the quasi-periodic route to chaos, remarked from  $E_3$  to  $E_2$  by black dashed circles,  $[0.58;0.84;0.61;0.66]$ .

In all cases analyzed, the values of TE present a maximum statistical significance (pvalue=0).

## Total Information flows and the functional invariant

Next, we have measured the total information flow, defined as the total outward of Transfer Entropy arriving to one enzyme minus the total inward. Positive values mean that that enzyme is a source of causality flow and negative flows are interpreted as sinks or targets. The results of the total information flows are shown in Table II (pvalue=0). The maximum source of total transfer information (0.41) corresponds to the  $E_2$  enzyme (phosphofructokinase) for  $A=0.021$ , when complex quasi-periodic oscillations appear in the glycolytic system.

For all conditions the enzyme  $E_2$  (phosphofructokinase) is the main source of effective influence and the enzyme  $E_3$  (pyruvatekinase) a sink, which could be interpreted as a target from a point of view based on its effective functionality. The enzyme  $E_1$  (hexokinase) is less constrained, and it has a flow close to zero for all conditions.

The attributed role to each enzyme, namely  $E_2$  the source,  $E_3$  the sink and  $E_1$  no-constrained is an invariant and preserved trough the whole route to chaos.

## Functional Synchronization

Time correlations allows for quantification about how much two time series are statistically independent. According to that, we have measured the time pairwise correlations in the enzymatic system, and the corresponding results are shown in Table III. The main finding is that  $E_2$  and  $E_3$  are highly synchronized (correlation=0.90, pvalue=0) and  $E_1$  is anti-synchronized with both  $E_2$  and  $E_3$  (respectively, correlation equals -0.65 and -0.66, pvalue=0).

These values of time correlations were almost constant trough the quasi-periodic route to chaos and established that the activities of  $E_2$  and  $E_3$  are grouped to the same function, being activated at similar time and oppositely to  $E_1$ .

## Redundancy and uncertainty reduction

The Mutual Information (MI) quantifies how much the knowledge of one variable reduces the entropy or uncertainty of the another [28]. The analysis of the glycolytic data by means of this method are shown in Table IV.

The high values of MI (close to 0.50) proved a high informative redundancy between the pairs of enzymes. So, the number of bits of information transferred from one enzyme to another is much larger than the actually needed.

The values in the principal diagonal of Table IV represent the uncertainty for each variable. We have found these values gradually descending,  $H(E_1)=[1.00;1.00;1.00;1.00]$ ,  $H(E_2)=[0.85;0.84;0.85;0.86]$  and  $H(E_3)=[0.76;0.74;0.76;0.78]$ , which is indicative of the uncertainty in the enzymatic activity patterns belonging to  $E_1$ ,  $E_2$  and  $E_3$  is reduced monotonously for all analyzed conditions.

The values of MI have a maximum statistical significance (pvalue=0).

Finally, we have computed the Mutual Information between the glucose input fluxes and the activity patterns of the different enzymes. In all cases, the MI was equal to zero, proving that the oscillations of the glucose were statistical independent of the glucose- 6-phosphate, fructose 1-6-biphosphate and pyruvate, products of the main irreversible enzymes of glycolysis.

## Discussion

In this paper we have quantified essential aspects of the effective functional connectivity among the main glycolytic enzymes in dissipative conditions.

First, we have computed under different source of glucose the causality flows in the metabolic system. This level of the functional influence accounts for the contribution of each enzyme to the generation of the different catalytic behavior and adds a directionality in the influence interactions between enzymes.

The results show that the flows of functional connectivity change significantly during the different metabolic transitions analyzed, exhibiting high values of transfer entropy, and in all considered cases, the enzyme phosphofructokinase ( $E_2$ ) is the main source of effective causality flow; the pyruvatekinase ( $E_3$ ) is the main sink of information flow; the hexokinase ( $E_1$ ) has a quasi-zero flow, meaning that, the total information arriving to  $E_1$  goes out to either  $E_2$  or  $E_3$ .

The maximum source of total transfer information (0.41) corresponds to the  $E_2$  enzyme (phosphofructokinase) at the edge of chaos, when complex quasi-periodic oscillations emerge (cf. Fig. 2). This finding seems to be consistent with other studies which show that when a dynamical system operates in the frontier between order (periodic behavior) and chaos its complexity is maximal [35,36].

The level of influence in terms of causal interactions between the enzymes is not always the same but varies depending on the substrate fluxes and the dynamic characteristics emerging in the system. In addition to the glycolytic topological structure characterized by the specific location of enzymes, substrates, products and regulatory metabolites there is an functional structure of information flows which is dynamic and exhibit notable variations of the causal interactions.

Another aspect of the glycolytic functionality was observed during the quantification of the Mutual Information, which measures how much the uncertainty about the one enzyme is reduced by knowing the other; we found that the uncertainty for  $E_1$ ,  $E_2$  and  $E_3$  monotonously decreased for all the values of the periodic glucose input-flux.

Second, the numerical results show that for all analyzed cases the maximum effective connectivity corresponds to the Transfer Entropy from  $E_2$  to  $E_3$ , indicating the biggest information flow in the multi-enzyme instability-generating system. This is also corroborated by the measure of correlation between the different pairs of series which shows that  $E_2$  and  $E_3$  are highly correlated, or synchronized (correlation=0.90 pvalue=0) and  $E_1$  is anti-correlated with both  $E_2$  and  $E_3$  (respectively, correlation=-0.65

pvalue=0 and correlation=-0.66 pvalue=0). The values of time correlations establish that the activities of  $E_2$  and  $E_3$  are grouped to the same function, being activated at similar time and oppositely to  $E_1$ .

Third, our analysis allows for a hierarchical classification in terms of what glycolytic enzyme is improving the future prediction of what others, and the results reveals in a quantitative manner that the enzyme  $E_2$  (phosphofructokinase) is the major source of causal information and represents the key-core of glycolysis. The second in importance is the  $E_3$  (pyruvatekinase).

From the biochemical point of view the  $E_2$  (phosphofructokinase) has been commonly considered as a major checkpoint in the control of glycolysis [37,38]. The main reason for this generalized belief is that this enzyme exhibits a complex regulatory behavior that reflects its capacity to integrate many different signals [39]; from a dissipative point of view, this enzyme catalyzes a reaction very far from equilibrium and its self-catalytic regulation it has been considered the main instability-generating mechanism for the emergence of oscillatory patters in glycolysis [6]. The functional studies presented here confirm in a quantitative manner that the  $E_2$  (phosphofructokinase) is the key-core of the pathway, and our results make stronger and expand the classical biochemical studies of glycolysis.

Forth, the dynamics of the glycolytic system changes substantially trough the quasi-periodic route to chaos when the amplitude of the input-flux varies. However, the hierarchy obtained by transfer entropy,  $E_2$  the flow,  $E_3$  the sink and  $E_1$  a quasi-zero flow, is preserved during this route and seems to be an invariant. This functional invariant of a metabolic process may be important for the understanding of functional enzymatic constraints in cellular conditions; but this issue requires other additional studies.

Finally, we want to emphasize that Transfer Entropy as a quantitative measure of effective causal connectivity can be a very useful tool in studies of enzymatic processes that operate far from equilibrium conditions. Moreover, many experimental observations have shown that the oscillations in the enzymatic activity seem to represent one of the most striking manifestations of the metabolic dynamic behaviors, of not only qualitative but also quantitative importance in cells (further details in Appendix III).

Transfer Entropy is able to detect the directed exchange of causality flows among the irreversible enzymes which might allow for a rigorous quantification of the effective functional connectivity of many dissipative metabolic processes in both normal and pathological cellular conditions.

The TE method applied to our numerical studies of yeast glycolysis shows the emergence of a new kind of dynamical functional structure which is characterized by changing connectivity flows and a metabolic invariant that constrains the activity of the irreversible enzymes.



The understanding the effective connectivity of the metabolic dissipative structures is crucial to address the functional dynamics of cellular life.

## Methods

### Model

In Fig. 1 are represented the main enzymatic processes of yeast glycolysis (the irreversible stages) with the enzymes arranged in series. When the metabolite S (glucose) feeds the system, it is transformed by the first enzyme  $E_1$  (hexokinase) into the product  $P_1$  (glucose-6-phosphate). The enzymes  $E_2$  (phosphofructokinase) and  $E_3$  (pyruvatekinase) are allosteric, and transform the substrates  $P'_1$  (fructose 6-phosphate) and  $P'_2$  (phosphoenolpyruvate) in the products  $P_2$  (fructose 1-6-bisphosphate) and  $P_3$  (pyruvate), respectively. The step  $P_2 \rightarrow P'_2$  represents reversible activity processes, reflected in the dynamic system by the functional variable  $\beta'$ . A part of  $P_1$  does not continue in the metabolic system, and is removed with a rate constant of  $q_1$  which is related with the activity of pentose phosphate pathway; likewise,  $q_2$  is the rate constant for the sink of the product  $P_3$  which is related with the activity of pyruvate dehydrogenase complex.

The main instability-generating mechanism in yeast glycolysis is the self-catalytic regulation of the enzyme  $E_2$  (phosphofructokinase), specifically, the positive feed-back exerted by the reaction products, the ADP and fructose-1,6-bisphosphate [3,5,6]. From a strictly biochemical point of view,  $E_2$  is also considered the main regulator enzyme of glycolysis [39]. The second irreversible stage for its regulatory importance is catalyzed by the enzyme  $E_3$  (pyruvatekinase) which is inhibited by the ATP reaction product [39]. Finally, the third irreversible process corresponds to the first stage the enzyme  $E_1$  (hexokinase) which is dependent on the ATP.

In the determination of the enzymatic kinetics of the enzyme  $E_1$  (hexokinase) the equation of the reaction speed dependent on glucose and ATP has been used [24]. The speed function of the allosteric enzyme  $E_2$  (phosphofructokinase) was developed in the framework of the concerted transition theory [3]. The reaction speed of the enzyme  $E_3$  (pyruvatekinase), dependent on ATP and phosphoenolpyruvate, was also constructed on the allosteric model of the concerted transition [25].

To study the kinetics of the dissipative glycolytic system we have considered normalized concentrations;  $\alpha$ ,  $\beta$  and  $\gamma$  denoted respectively the normalized concentrations of  $P_1$ ,  $P_2$  and  $P_3$ . For a spatially

homogeneous system the time-evolution is described by the following three delay differential equations:

$$\begin{aligned}
\frac{d\alpha}{dt} &= z_1\sigma_1\phi_1(\mu) - \sigma_2\phi_2(\alpha, \beta) - q_1\alpha \\
\frac{d\beta}{dt} &= z_2\sigma_2\phi_2(\alpha, \beta) - \sigma_3\phi_3(\beta, \beta', \mu) \\
\frac{d\gamma}{dt} &= z_3\sigma_3\phi_3(\beta, \beta', \mu) - q_2\gamma
\end{aligned} \tag{1}$$

where the functional variables  $\beta'$  and  $\mu$  reflect the normalized concentrations of  $P'_2$  (phosphoenolpyruvate) and ATP respectively. The three main enzymatic functions are the following:

$$\begin{aligned}
\phi_1(\mu) &= \frac{\mu SK_{d3}}{(K_3K_2 + \mu K_{m1}K_{d3} + SK_2 + \mu SK_{d3})} \\
\phi_2(\alpha, \beta) &= \frac{\alpha(1+\alpha)(1+d_1\beta)^2}{L_1(1+c\alpha)^2 + (1+\alpha)^2(1+d_1\beta)^2} \\
\phi_3(\beta, \beta', \mu) &= \frac{d_2\beta'(1+d_2\beta')^3}{L_2(1+d_3\mu)^4 + (1+d_2\beta)^4}
\end{aligned} \tag{2}$$

and

$$\begin{aligned}
\beta' &= f(\beta(t - \lambda_1)) \\
\mu &= h(\beta(t - \lambda_2)).
\end{aligned} \tag{3}$$

The constants  $\sigma_1$ ,  $\sigma_2$  and  $\sigma_3$  correspond to the maximum activity of  $E_1$ ,  $E_2$  and  $E_3$  ( $V_{m1}$ ,  $V_{m2}$  and  $V_{m3}$ ) divided by the Michaelis constants of each enzyme, respectively  $K_{m1}$ ,  $K_{m2}$  and  $K_{m3}$ . The constants  $z$ 's are defined as  $z_1 = K_{m1}/K_{m2}$ ,  $z_2 = K_{m2}/K_{m3}$  and  $z_3 = K_{m3}/K_{d3}$ , with  $K_{d3}$  representing the dissociation constant of  $P_2$  by  $E_3$ . The constants  $d$ 's are  $d_1 = K_{m3}/K_{d2}$ ,  $d_2 = K_{m3}/K_{d3}$  and  $d_3 = K_{d3}/K_{d4}$ , with  $K_{d4}$  representing the dissociation constant of ATP;  $L_1$  and  $L_2$  are respectively the allosteric constant of  $E_2$  and  $E_3$ ;  $c$  is the non-exclusive binding coefficient of the substrate  $P_1$ . More details about parameter values and experimental references are given in Appendix I.

From the dissipative point of view the essential enzymatic stages are those that correspond to the biochemical irreversible processes [40] and to simplify the model, we did not consider the intermediate part of glycolysis belonging to the enzymatic reversible stages. In this way, the functions  $f$  and  $h$  are

supposed to be the identity function. Thus,

$$\begin{aligned}\beta' &= \beta(t - \lambda_1) \\ \mu &= \gamma(t - \lambda_2)\end{aligned}\tag{4}$$

The initial functions present a simple harmonic oscillation in the following form:

$$\begin{aligned}\alpha_0(t) &= A + B \sin(2\pi/P) \\ \beta_0(t) &= C + D \sin(2\pi/P) \\ \gamma_0(t) &= E + F \sin(2\pi/P)\end{aligned}\tag{5}$$

with  $A = 26$ ,  $B = 12$ ,  $C = 12$ ,  $D = 10$ ,  $E = 7$ ,  $F = 6$  and  $P = 534$ .

The dependent variables  $\alpha$ ,  $\beta$  and  $\gamma$  were normalized dividing them by  $K_{m2}$ ,  $K_{m3}$  and  $K_{d3}$ , and the parameters  $\lambda_1$  and  $\lambda_2$  are time delays affecting the independent variable (see for more details the Appendix II).

The numerical integration of the system was performed with the package ODE Workbench, which created by Dr. Aguirregabiria is part of the Physics Academic Software. Internally this package uses a Dormand-Prince method of order 5 to integrate differential equations. Further information at <http://www.webassign.net/pas/ode/odewb.html>.

This model has been exhaustively analyzed before, revealing a notable richness of emergent temporal structures which included the three main routes to chaos, as well as a multiplicity of stable coexisting states, see for more details [26, 32, 33].

## Transfer Entropy

TE allows for a quantification of how much the temporal evolution of the activity of one enzyme helps to improve the future prediction of another. The oscillatory patterns of the biochemical metabolites might have information which can be read-out by the TE.

For a convenient derivation, let generally assume that each of the pairs of enzymatic activity is represented by the two time series  $X \equiv \{x_t\}_{t=1}^T$  and  $Y \equiv \{y_t\}_{t=1}^T$ . Here,  $x_t$  is the state value of the variable  $X$  in time  $t$ , and similarly for  $y_t$ . Let  $I(X^P, Y^P \rightarrow X^F) = -\sum_{x_{t+1}, x_t, y_t} P(x_{t+1}, x_t, y_t) \log_2 P(x_{t+1}|x_t, y_t)$

be the amount of information required to predict the future of  $X$  ( $X^F$ ) known both the pasts of  $X$  and  $Y$  ( $X^P$  and  $Y^P$ ). Analogously, let  $I(X^P \rightarrow X^F) = -\sum_{x_{t+1}, x_t} P(x_{t+1}, x_t) \log_2 P(x_{t+1}|x_t)$  be the amount of information required to predict the future of  $X$  known only its past. The difference  $I(X^P \rightarrow X^F) - I(X^P, Y^P \rightarrow X^F)$  is by definition the transfer entropy from  $Y$  to  $X$ , denoted by  $TE_{Y \rightarrow X}$ . It quantifies the amount of information in digits that  $Y$  adds to the predictability of  $X$ .

Rewriting the conditional probabilities as the joint probability divided by its marginal, one obtains an explicit form for the Transfer Entropy:

$$TE_{Y \rightarrow X} = \sum_{x_{t+1}, x_t, y_t} P(x_{t+1}, x_t, y_t) \log_2 \left( \frac{P(x_{t+1}, x_t, y_t) P(x_t)}{P(x_t, y_t) P(x_{t+1}, x_t)} \right). \quad (6)$$

The formula (6) is fully equivalent to the Mutual Information between  $X^F$  and  $Y^P$  conditioned to  $X^P$ . Thus,  $TE_{Y \rightarrow X} \equiv I(X^F, Y^P | X^P)$ , and consequently, Transfer Entropy says about how much information the inclusion of  $Y^P$  adds to the prediction of  $X^F$  only considering  $X^P$ , ie.  $I(X^F, Y^P | X^P) = H(X^F | X^P) - H(X^F | X^P, Y^P)$ . Therefore, TE is fully quantifying the information flows between pairs of variables. The values of TE were normalized between 0 and 1.

It is important to remark that the TE from  $X$  to  $Y$  is different to the one from  $Y$  to  $X$ , ie. the effective connectivity is asymmetric, adding a directionality in time which accounts for a particular case of *directed graphs*, the graph of information flows between pairs of enzymes.

Alternatively to the Transfer Entropy, effective connectivity can be obtained using Granger Causality [41], which makes emphasis on how much from the past of one variable the predictability of its future is improved by adding the past of another variable. Recently, it has been proved that in the case of Gaussian variables both Transfer Entropy and Granger Causality are measuring exactly the same [42]. Therefore, the information flows based on Transfer Entropy and the Granger causality interactions coincide for Gaussian variables.

## Mutual Information and Redundancy

MI quantifies how much the knowledge of one variable reduces the entropy or uncertainty of another. Therefore, MI says about how much information the two variables are sharing. The strongest point of the MI is that it extends functionality to high order statistics [28]. Its definition is  $MI(X, Y) =$

$H(X) - H(X|Y)$ , where  $H(X|Y) = H(X, Y) - H(Y)$  is the conditional entropy of  $X$  given  $Y$ . It accounts for the remaining uncertainty in  $X$  knowing the variable  $Y$ . We referred  $H(X)$  and  $H(X, Y)$  as respectively the joint and marginal (Shanon) entropies.

For statistical independent  $X$  and  $Y$  variables one has  $MI(X, Y) = 0$ . The other limit satisfies  $MI(X, X) = H(X)$ , because of  $H(X|Y) = 0$ . Therefore, the MI of two variables is bounded and satisfies that  $0 \leq MI(X, Y) \leq H(X)$ . High values of MI mean that the redundancy in information between the two variables is large. The values of MI were normalized between 0 and 1.

## Number of bins vs Statistical significance

For all the probabilities used in both Transfer Entropy (TE) and Mutual Information (MI) we used a number of bins of 10. As it is well-known, the calculation of these probabilities is sensitive to the number of bins. Instead of tuning it as a control parameter to compute the probabilities, we preferred explored the statistical significance of the computed values. This was achieved by comparing both the TE and MI between the two series of enzymatic activity, say  $X$  and  $Y$ , with the values obtained when considering a random permutation of  $Y$ , what we called, the shuffled  $Y$ . The values of both TE and MI shown in Tables I and III were larger than those calculated in the shuffled situation (for both TE and MI, pvalue=0, for 50 different samples).

## Acknowledgments

JMC is funded by the Spanish Ministerio de Ciencia e Innovacion, programa Ramon y Cajal, and from Junta de Andalucia, grants P09-FQM-4682 and P07-FQM-02725. I.M. De la Fuente acknowledges useful advises and suggestions from Prof. J. Vaguillas.

## References

1. Duysens L, Ames J (1957) Fluorescence spectrophotometry of reduced phosphopyridine nucleotide in intact cells in the near-ultraviolet and visible region. *Biochem Biophys Acta* 24: 19-26.
2. Chance B, Hess B, Betz A (1964) DPNH oscillations in a cell-free extract of *S. carlsbergensis*. *Biochem Biophys Res Commun* 16: 182-187.
3. Goldbeter A, Lefebvre R (1972) Dissipative structures for an allosteric model. *Biophys J* 12: 1302-1315.
4. Goldbeter A, Lefebvre R (1973) Patterns of spatiotemporal organization in an allosteric enzyme model. *Proc Natl Acad Sci USA* 70: 3255-3259.
5. Boiteux A, Goldbeter A, Hess B (1975) Control of oscillating glycolysis of yeast by stochastic, periodic, and steady source of substrate: a model and experimental study. *Proc Natl Acad Sci USA* 72: 3829-3833.
6. Goldbeter A (2007) Biological rhythms as temporal dissipative structures. *Advances in Chemical Physics* 135: 253-295.
7. Bagheri S, Nosrati M, Li S, Fong S, Torabian S, et al. (2006) Genes and pathways downstream of telomerase in melanoma metastasis. *Proc Natl Acad Sci USA* 103: 11306-11311.
8. Almeida A, Bolaos J, Moncada S (2010) E3 ubiquitin ligase APC/C-Cdh1 accounts for the Warburg effect by linking glycolysis to cell proliferation. *Proc Natl Acad Sci USA* 107: 7387-7391.
9. Vlassenko A, Vaishnavia S, Couture L, Sacco D, Shannona B, et al. (2010) Spatial correlation between brain aerobic glycolysis and amyloid- $\beta$  ( $A\beta$ ) deposition. *Proc Natl Acad Sci USA* : [www.pnas.org/cgi/doi/10.1073/pnas.1010461107](http://www.pnas.org/cgi/doi/10.1073/pnas.1010461107).
10. Garriga-Canut M, Schoenike B, Qazi R, Bergendahl K, Daley T, et al. (2006) 2-Deoxy-D-glucose reduces epilepsy progression by NRSF-CtBP-dependent metabolic regulation of chromatin structure. *Nat Neurosci* 9: 1382-1387.

11. Colussi C, Albertini M, Coppola S, Rovidati S, Galli F, et al. (2006) H<sub>2</sub>O<sub>2</sub>-induced block of glycolysis as an active ADP-ribosylation reaction protecting cells from apoptosis. *FASEB J* 14: 2266-2276.
12. Danial N, Gramm C, Scorrano L, Zhang C, Krauss S, et al. (2003) BAD and glucokinase reside in a mitochondrial complex that integrates glycolysis and apoptosis. *Nature* 424: 952-956.
13. Termonia Y, Ross J (1981) Oscillations and control features in glycolysis: Numerical analysis of a comprehensive models. *Proc Natl Acad Sci USA* 78: 2952-2956.
14. Dano S, Sorensen P, Hynne F (1999) Sustained oscillations in living cells. *Nature* 402: 320-322.
15. Wolf J, Passarge J, Somsen O, Snoep J, Heinrich R, et al. (2000) Transduction of intracellular and intercellular dynamics in yeast glycolytic oscillation. *Biophys J* 78: 1145-1153.
16. Reijenga K, Westerhoff H, Kholodenko B, Snoep J (2002) Control analysis for autonomously oscillating biochemical networks. *Biophys J* 82: 99-108.
17. Madsen MF, Dano S, Sorensen PG (2005) On the mechanisms of glycolytic oscillations in yeast. *FEBS J* 272: 2648-2660.
18. Olsen L, Andersen A, Lunding A, Brasen J, Poulsen A (2009) Regulation of Glycolytic Oscillations by Mitochondrial and Plasma Membrane H<sup>+</sup>-ATPases. *Biophys J* 96: 3850-3861.
19. Gerstein G, Perkel D (1969) Simultaneously recorded trains of action potentials: analysis and functional interpretation. *Science* 164: 828-830.
20. Friston K (1994) Functional and effective connectivity in neuroimaging: A synthesis. *Hum Brain Mapping* 2: 56-78.
21. Fujita A, Sato J, Garay-Malpartida H, Morettin P, Sogayar M, et al. (2007) Time-varying modeling of gene expression regulatory networks using the wavelet dynamic vector autoregressive method. *Bioinformatics* 23: 1623-1630.
22. Mukhopadhyay N, Chatterjee S (2007) Causality and pathway search in microarray time series experiment. *Bioinformatics* 23: 442-449.

23. Pahle J, Green A, Dixon C, Kummer U (2008) Information transfer in signaling pathways: a study using coupled simulated and experimental data. *BMC Bioinformatics* 9: 139.
24. Viola E, Raushel M, Rendina R, Cleland W (1982) Substrate synergism and the kinetic mechanism of yeast hexokinase. *Biochem* 21: 1295-1302.
25. Markus M, Plessner T, Boiteux A, Hess B, Malcovati M (1980) Rate law of pyruvate kinase type I from *Escherichia coli*. *Biochem J* 189: 421-433.
26. De la Fuente IM, Martinez L, Veguillas J, Aguirregabiria J (1996) Quasiperiodicity route to chaos in a biochemical system. *Biophys J* 71: 2375-2379.
27. Schreiber T (2000) Measuring information transfer. *Phys Rev Lett* 85: 461-464.
28. Cover T, Thomas J (1991) *Elements of Information Theory*. New York: John Wiley & Sons, Inc.
29. Markus M, Muller S, Hess B (1985) Observation of entrainment quasiperiodicity and chaos in glycolyzing yeast extracts under periodic glucose input. *Ber Bunsen-Ges Phys Chem* 89: 651-654.
30. Markus M, Kuschmitz D, Hess B (1985) Properties of strange attractors in yeast glycolysis. *Biophys Chem* 22: 95-105.
31. Markus M, Kuschmitz D, Hess B (1984) Chaotic Dynamics in Yeast Glycolysis Under Periodic Substrate Input Flux. *FEBS* 172: 235-238.
32. De la Fuente IM (1999) Diversity of temporal self-organized behaviors in a biochemical system. *BioSystems* 50: 83-97.
33. De la Fuente IM, Martinez L, Veguillas J (1996) Intermittency route to chaos in a biochemical system. *Biosystems* 39: 87-92.
34. Ruelle D, Takens F (1971) On the nature of turbulence. *Commun Math Phys* 20: 167-172.
35. Kaufmann S, S (1991) Coevolution to the edge of chaos: Coupled fitness landscapes, poised states, and coevolutionary avalanches. *J Theo Biol* 149: 467-505.
36. Bertschinger N, Natschlager T (2004) Real-Time Computation at the Edge of Chaos in Recurrent Neural Networks. *Neural Comput* 16: 1413-1436.



37. Serrano G (1989) *The Yeasts*. London: Academic Press.
38. JJ Heinisch EB, Timpel C (1996) A yeast phosphofructokinase insensitive to the allosteric activator fructose-2,6-bisphosphate. *J Biol Chem* 271: 15928-15933.
39. Stryer L (1995) *Biochemistry*. New York: W.H. Freeman.
40. Ebeling W, Engel-Herbert H, Herzel H (1986) Thermodynamic aspects of selforganization. In *Selforganization by Nonlinear Irreversible Processes*. Berlin: Springer-Verlag, pp. 2-16.
41. Granger C (1969) Investigating causal relations by econometric models and cross-spectral methods. *Econometrica* 37: 424-438.
42. Barnett L, Barrett A, Seth A (2009) Granger causality and transfer entropy are equivalent for gaussian variables. *Phys Rev Lett* 103: 238701.

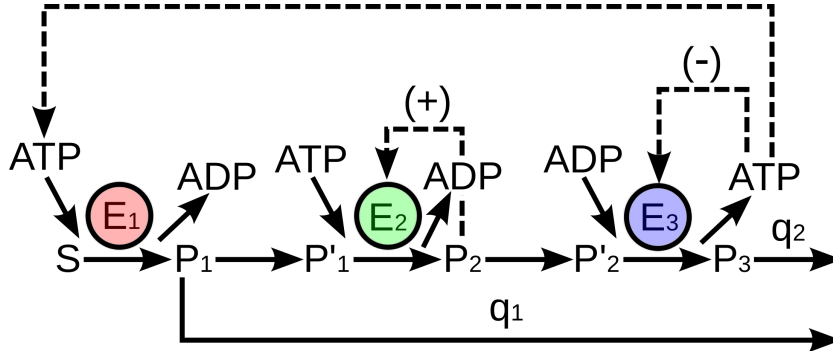


**Figure 1. Multi-enzyme instability-generating system of yeast glycolysis.** The main irreversible enzymatic processes are arranged in series:  $E_1$  (hexokinase),  $E_2$  (phosphofructokinase) and  $E_3$  (pyruvatekinase).  $S$ ,  $P_1$ ,  $P'_1$ ,  $P_2$ ,  $P'_2$  and  $P_3$  denote, respectively, the concentrations of glucose, glucose-6-phosphate, fructose 6-phosphate, fructose 1,6-bisphosphate, phosphoenolpyruvate and pyruvate.  $q_1$  is the rate first-order constant for the removal of  $P_1$ ;  $q_2$  is the rate constant for the sink of the product  $P_3$ . The model includes the feedback activation of  $E_2$  and the feedback inhibition of  $E_3$ . The ATP is consumed by  $E_1$  and recycled by  $E_3$ .

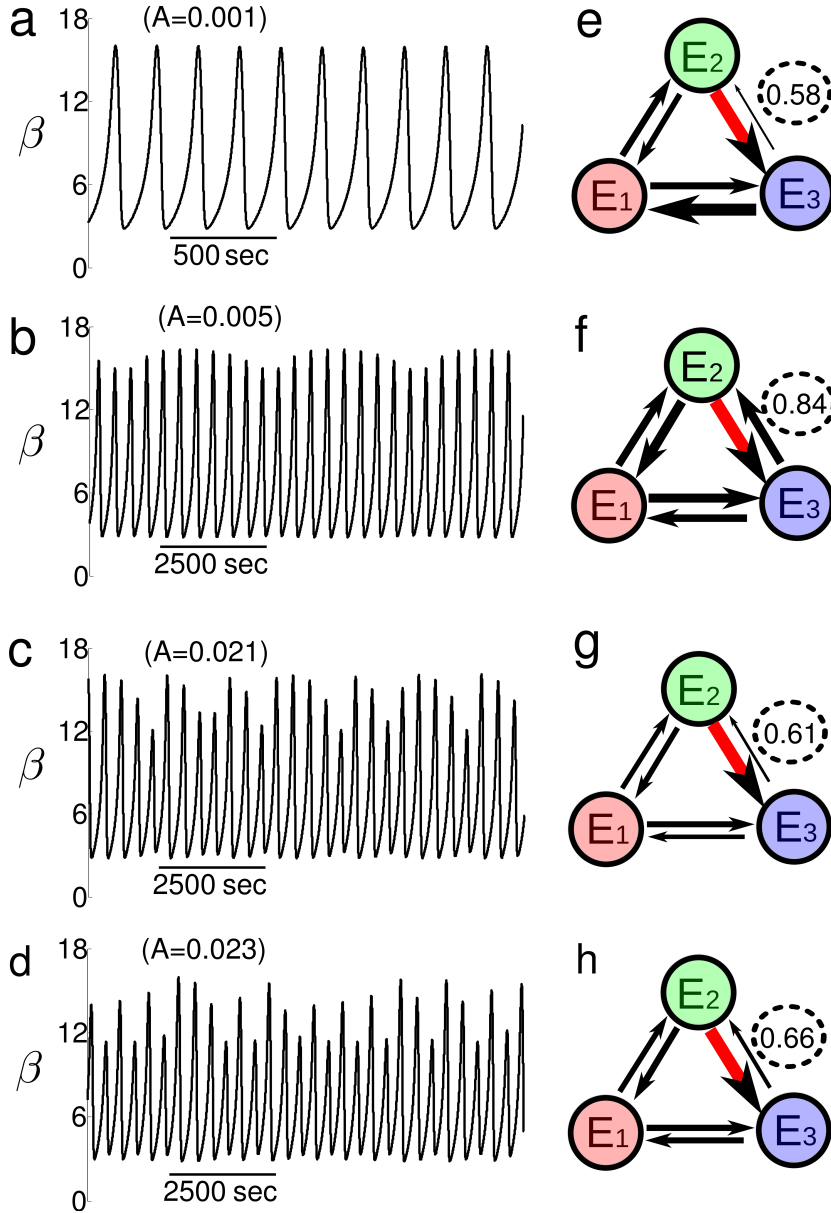


**Figure 2. Glycolytic route to chaos and dynamical effective connectivity.** Left Panel: The time evolution of the  $E_2$  activity (the normalized concentration  $\beta$ , fructose 1,6-bisphosphate) shows a quasi-periodic route to chaos when varying the amplitude of the periodic input-flux from  $A=0.001$  (top) to  $A=0.023$  (bottom). (a) Periodic pattern. (b) Quasi-periodic oscillations. (c) Complex quasi-periodic motion indicating the beginning destruction of the periodic behavior. (d) Deterministic chaos. All series are plotted after 10000 seconds. Right Panel: Effective connectivity of the system for the same values of  $A$  in the left panel. The strength of effective connectivity is plotted with arrows width proportional to the Transfer Entropy divided by the maximum value (red arrow), cf. results given in Table I. Black dashed circles at the TE from  $E_3$  and  $E_2$  emphasize that the strength of Information flows is not the same, but varies through the quasi-periodic route to chaos.

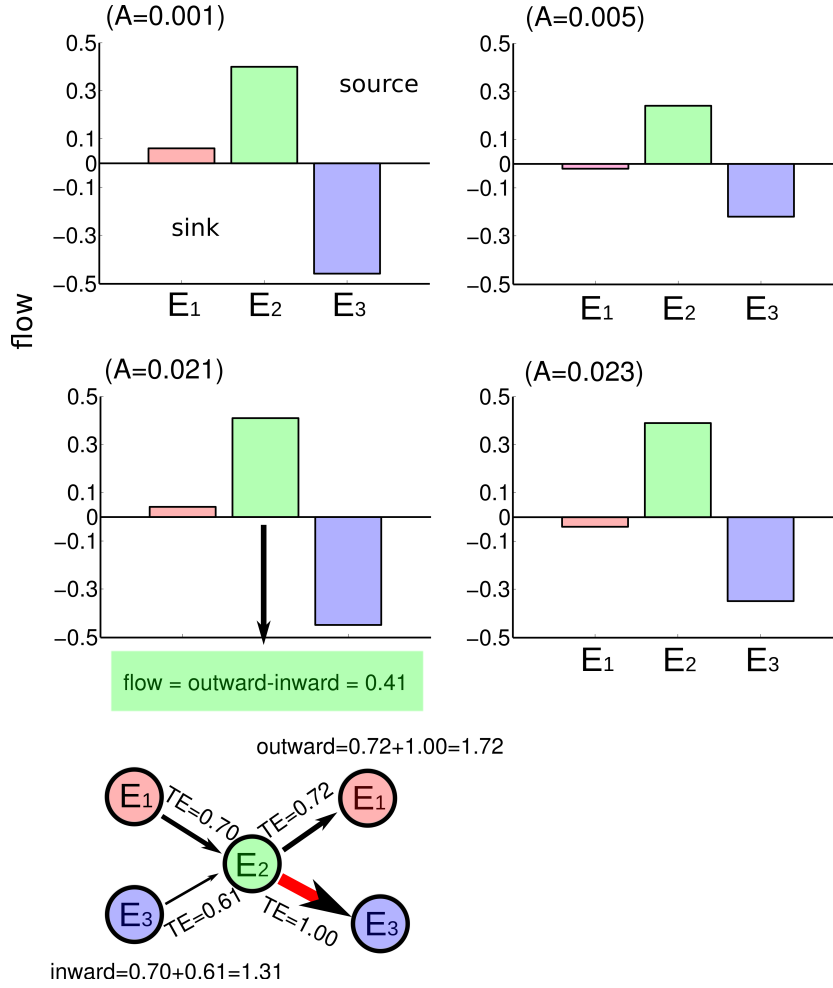


**Figure 3. Total information flows and the functional invariant.** Bars represent the total information flow, defined per each enzyme as the total outward TE minus the total inward. For  $A=0.021$  and  $E_2$  an schematic visualization of the calculation of this flow is shown (bottom graph of the panel). The functionality attributed for each enzyme is an invariant and preserved along the route, ie.  $E_2$  is a source,  $E_3$  is a sink and  $E_1$  has a quasi-zero flow.

## Tables

Table I. Values of normalized Transfer Entropy

	From $E_1$	From $E_2$	From $E_3$
To $E_1$	—	[0.73;0.88;0.72;0.76]	[0.74;0.80;0.68;0.74]
To $E_2$	[0.76;0.80;0.70;0.72]	—	[0.58;0.84;0.61;0.66]
To $E_3$	[0.78; 0.86;0.74;0.75]	[1.00;1.00;1.00;1.00]	—

Table II. Values of total information flows

$\mathbf{E}_1$	[0.06; -0.02;0.04;-0.04]	Quasi-zero flow
$\mathbf{E}_2$	[0.40; 0.24;0.41;0.39]	source
$\mathbf{E}_3$	[-0.46; -0.22;-0.45;-0.35]	sink

Table III. Time Correlations

	$\mathbf{E}_1$	$\mathbf{E}_2$	$\mathbf{E}_3$
$\mathbf{E}_1$	[1.00;1.00;1.00;1.00]	[-0.65;-0.66;-0.64;-0.63]	[-0.66;-0.66;-0.66;-0.66]
$\mathbf{E}_2$	[-0.65;-0.66;-0.64;-0.63]	[1.00;1.00;1.00;1.00]	[0.90;0.90;0.90;0.90]
$\mathbf{E}_3$	[-0.66;-0.66;-0.66;-0.66]	[0.90;0.90;0.90;0.90]	[1.00;1.00;1.00;1.00]

Table IV. Values of normalized Mutual Information

	$\mathbf{E}_1$	$\mathbf{E}_2$	$\mathbf{E}_3$
$\mathbf{E}_1$	[1.00;1.00;1.00;1.00]	[0.52;0.49;0.45;0.44]	[0.48;0.49;0.45;0.44]
$\mathbf{E}_2$	[0.52;0.49;0.45;0.44]	[0.85;0.84;0.85;0.86]	[0.47;0.46;0.45;0.45]
$\mathbf{E}_3$	[0.48;0.49;0.45;0.44]	[0.47;0.46;0.45;0.45]	[0.76;0.74;0.76;0.78]